6th IAHR International Meeting of the Workgroup on Cavitation and Dynamic Problems in Hydraulic Machinery and Systems, September 9-11, 2015, Ljubljana, Slovenia

NUMERICAL AND EXPERIMENTAL INVESTIGATIONS OF A HYDRAULIC PIPE DURING A GATE CLOSURE AT A HIGH REYNOLDS NUMBER

Olivier Petit*

Chalmers University of Technology, Division of Fluid Dynamics, Gothenburg

Chao Wang

Wuhan University, State Key Laboratory of Water Resources and Hydropower Engineering Science, Wuhan

Michel Cervantes

Luleå University of Technology, Division of Fluid and Experimental Mechanics, Luleå

James Yang

Royal Institute of Technology (KTH), Division of Hydraulic Engineering, Stockholm

Håkan Nilsson

Chalmers University of Technology, Division of Fluid Dynamics, Gothenburg

ABSTRACT

The role of hydropower to provide regulated power is important to the Swedish power system. This becomes even more accentuated with the expansion of intermittent renewable electricity sources, such as wind power. The variation of hydropower operation ranges over a large spectrum of time scales, from seconds to years. For scales larger than a minute, the flow may be considered as quasi-steady from a hydrodynamic point of view. The present work addresses the shorter time scales. Such scales are manifested mainly as pressure transients, which is an issue of concern in design and operation of hydropower plants.

The objective of the study is to address rapid pressure transients with a special focus on detailed 3D processes interacting with transients travelling in an essentially 1D geometry. The test case is a gate closing in a long rectangular pipe, where a high-Reynolds number flow is driven by a pressure difference between upper and lower water levels. Experimental time-resolved static pressure and PIV data are gathered for validation of the numerical results.

In a first stage the computational domain is modelled in 3D with an incompressible volume of fluid method that includes the prediction of the free surfaces. The domain includes the upper and lower water tanks with free water surfaces, a pipe in-between and a closing and opening gate. The gate movement is modelled with a dynamic mesh that removes the cells as the gate closes. The block-structured mesh is generated in ICEM CFD, and parallel simulations are performed using the OpenFOAM open source software. The numerical results are compared with the experimental data, and it is shown that the experimentally observed pressure fluctuations after gate closure are not an effect of the free surfaces.

In a second stage, the upper tank and the pipe are modelled using a compressible 1D code based on the method of characteristics (MOC). A comparison with the experimental data shows that the correct unsteady behavior of the system is captured by the 1D approach if the losses and the gate characteristics are correctly accounted for, at the same time as the compressibility is adapted to the air contents of the water and flexibility of the structure.

KEYWORDS

Transient flow, multiphase, hydraulic system, CFD, MOC, PIV.

* *Corresponding author:* Chalmers University of Technology, Fluid Dynamics Division, 41296 Gothenbourg, Sweden, phone: +46317725034, email: olivierp@chalmers.se

1. Introduction

During the peak period of hydropower development in Sweden, limitations of operations due to transients were usually determined by physical models or in less complex cases by handmade calculations. The basic theory and methods to predict pressure surges have been well documented in textbooks since long [1-4]. However, since several decades computer models dominate the analysis of more complex pressure surges. One-dimensionality is a fairly accurate representation of most waterway systems and is often used to model such systems. More complex components like bends, valves, gates, etc. may be represented by losses of a semi-empirical origin [5, 6]. Such 1D computations of transient flow phenomena have been used to address complex phenomena in sometimes complex systems [7-10]. If the complexity of the involved system components increases, full 3D modelling may be used.
In the present work the pressure surge following a rapidly gate closure is investigated. A test rig is designed and built to perform experimental analysis of the phenomena. The experimental data show pressure fluctuations when the gate is closed. To further understand those fluctuations, numerical simulations are performed and compared with the experimental data. In a first stage, the OpenFOAM open source CFD tool is used to study a 3D incompressible flow in the system. A minor loss is estimated and implemented in the 3D model to get the same pressure loss in the system as the one observed in the experiments. The free surfaces of the upstream and downstream tanks are included in the simulation to investigate their influences on the pressure fluctuations. In a second stage a 1D approach that takes into account a finite sound propagation speed is used to model the system. The minor pressure loss previously determined is implemented in the 1D model as well. The results show that the compressibility of the water and its mixture with air, as well as the flexibility of the structure, are likely to be the cause of the pressure fluctuations observed in the experiments.

2. Test rig and experimental investigations

The test rig shown in Figure 1 was built at Vattenfall R&D Laboratory. The flow is driven by the difference in elevation between the water surfaces in the upstream and downstream water tanks.

2.1. Design of test rig

The rig is mainly composed of an upstream and a downstream water tank, a 90º bend, a 10 m rectangular pipe and two knife valves, see Figure 1. The knife valve below the upstream tank limits the discharge when the second one (hereafter referred to as “gate“) is fully open. The upstream valve opening is fixed during the experiment and creates a minor loss that is proportional to the square of the velocity. The gate is closed linearly during 5 s, kept closed during 8 s and opened linearly during 5 s, to generate the transient process in the system. The upstream tank is continuously fed by water and the outlet of the downstream tank has constant properties throughout the measurement.
The rectangular pipe inner dimensions measure 200 mm (width) by 250 mm (height). It is constructed in plexi glass which is placed in an aluminum frame to guarantee its structural integrity. The gate is made of a sheet steel and is placed 8 m downstream the bend and 2 m upstream the downstream tank. The upper tank has a 1.27 m^2 water area while the downstream tank water area is 6 m^2. The water flows into the upstream tank at a rate of 50 $l.s^{-1}$, at which the system stabilizes to the fixed surface levels when the gate is fully open.

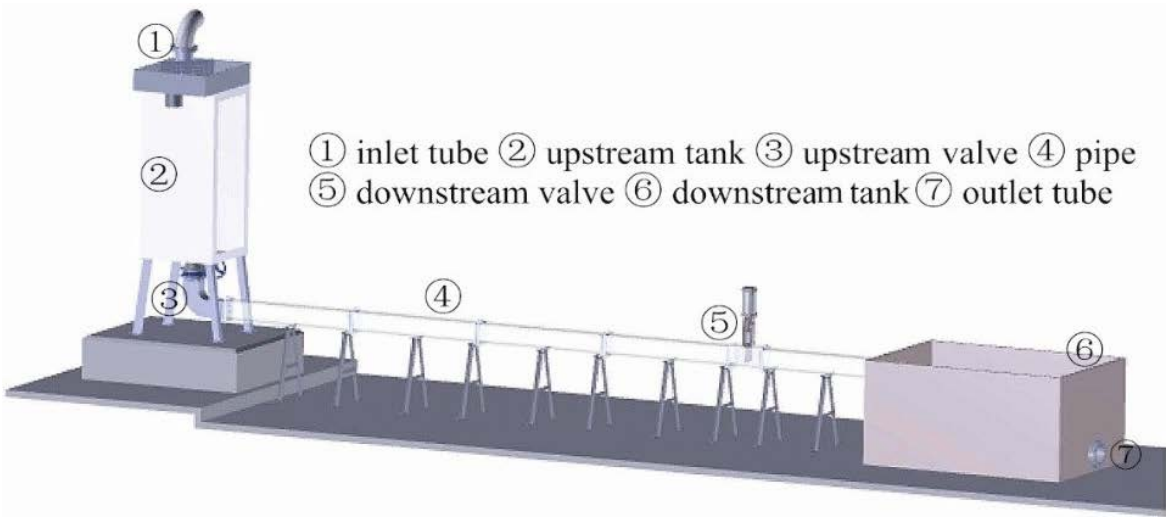

Figure 1: Layout of test rig

2.2. Experimental setup

During the experiments, the flow rate was maintained at a constant value of 50 $l.s^{-1}$, yielding a Reynolds number $Re=1.93 \cdot 10^5$ based on the hydraulic diameter Dh=222 mm and a water temperature of 15°C. Differential pressure sensors from Druck, PDCR 810, with two different measuring ranges (0-0.7 and 0-1 bar) were used. They have an accuracy of ±0.1%. The pressure taps were placed at cross-section 1 (hereafter referred to as "S1", 1.245 m upstream the gate) and at cross-section 2 (hereafter referred to as "S2", 3.245 m upstream the gate). Velocity measurements were performed with a particle image velocimetry system (PIV) from LaVision GmbH.
The PIV system, the data acquisition system recording the pressure signal, and the gate position were coupled enabling simultaneous measurements of the pressure, gate position and velocity as a function of time.

2.3. Experimental results

The pressure variation for the two sensors is presented in Figure 2. The main pressure variations occur as the gate closes from 5 s to 10 s, and opens from 18 s to 23 s. Oscillations in the pressure are present after complete closure, with a period of about 0.48 s. The damping of the oscillations is significant. The pressure oscillates about a mean level that increases linearly in time, corresponding to the constant flow into the upstream tank and the increase of the upstream surface elevation. These oscillations may be attributed to a water hammer effect, but the period of the oscillations is very large in relation to the length of the pipe and the sound propagation speed of pure water. The pressure oscillations may be as well attributed to standing waves formed in the upper tank. To further understand the pressure oscillations, the test case is numerically investigated in sections 3 and 4.
Figure 3 shows the gate opening as a function of time and the variation of the axial velocity 50 mm upstream the gate at the center of the pipe. The gate is fully opened at position 0 mm and fully closed at position 250 mm. The axial velocity is extracted from the PIV data shown in Figure 4. The curve is noisy since it is the instantaneous velocity. The flow being highly turbulent, the velocity curve is a combination of the mean value and the fluctuation at each time instant. As the gate starts to close, the velocity slightly increases from the steady-state 1 $m.s^{-1}$and does not decrease significantly until 2/3 of the gate is close. Figure 4 presents the variation of the axial velocity along a vertical line 50 mm upstream the gate, similarly to

Figure 3, but at a range of vertical locations measured from the upper wall. The gate starts to close at 5 s and is fully closed at 10 s.

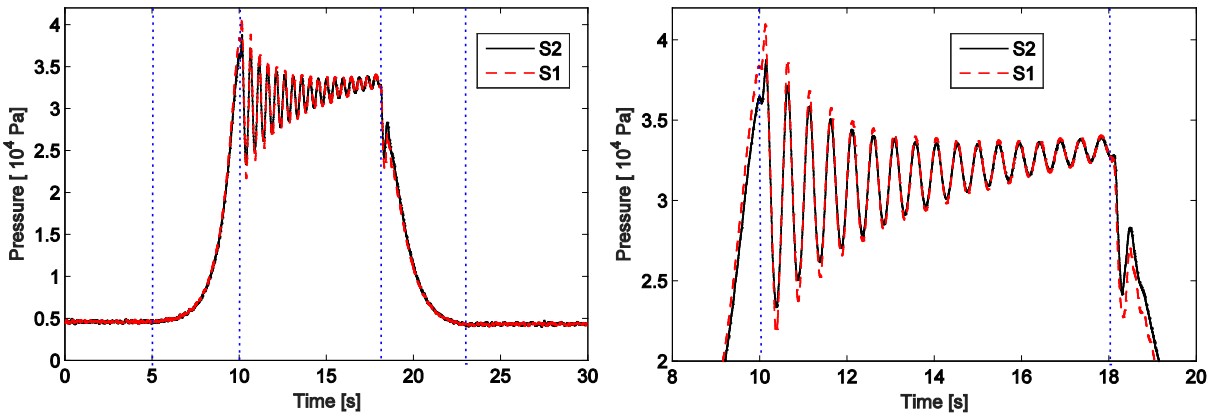

Figure 2: Pressure variation recorded at the two sensor positions upstream the gate.

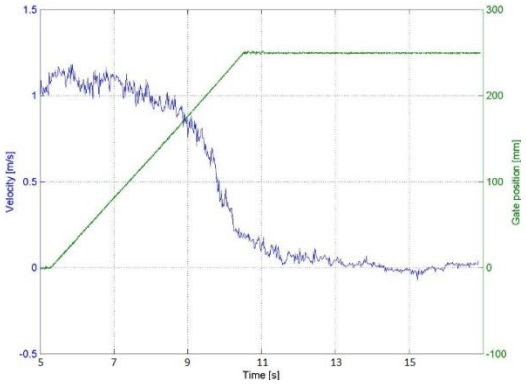

Figure 3: The gate closure function and the variation of the axial velocity in the center of the pipe, 50 mm upstream the gate.

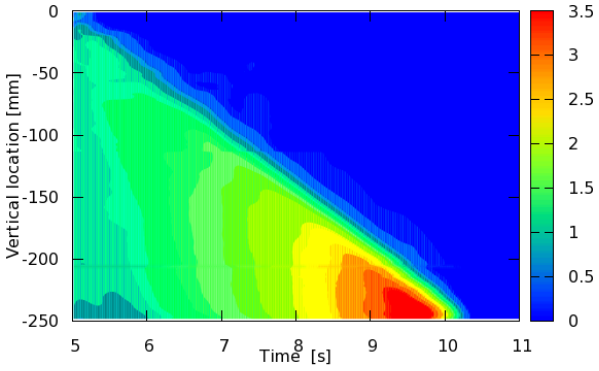

Figure 4: Variation of the axial velocity as a function of time along a vertical line 50 mm upstream the gate.

2.4. Minor loss determination

Both the entrance to the pipe and the knife valve below the upstream tank contribute to a minor-loss at this location. The minor-loss coefficient is here estimated from the experimental data. The energy equation between the water surface in the upstream tank (subscript 1), assuming $V_1 \approx 0$ and $p_1 = p_{ref}$, and a position in the pipe after the valve located below the upstream tank (subscript 2) yields

$$p_{ref} + \rho g h_1 = p_2 + \rho \frac{V_2^2}{2} + \rho g h_2 + k\rho \frac{V_2^2}{2},$$

where k is the minor-loss coefficient. The minor-loss is here assumed to appear in a region with the same cross-section area as the pipe, thus subscript 2 for the velocity in the last term. Here, p_{ref} is used instead of p_{atm}, since the experimental data is not reported in absolute values. With a closed gate ($V_2^2 = 0$), the total pressure in the pipe is given by $p_{0,2} = p_{ref} + \rho g(h_1 - h_2)$. This pressure can be estimated from the experimental results, as the mean value when the gate is closed (see Figure 2). Here it is estimated to $p_{0,2} = 30\ kPa$. With a fully open gate the flow rate ($50\ l.s^{-1}$) and the pipe cross-section area ($200 \times 250\ mm$) yields $V_2 \approx 1\ m.s^{-1}$, and the pressure in the pipe can be estimated from the experimental data as $p_2 = 5\ kPa$. Under these conditions the energy equation yields, assuming $\rho = 1000\ kg.m^{-3}$, a minor loss coefficient of $k = 49$.

2.5. Estimation of sound speed

The finite speed of sound in water creates a phase shift between the signals recorded by the two pressure probes, see Figure 2. The attenuation of the wave is clear while the phase shift is very small. A cross-correlation of the signals allows a determination of the time delay and thus the wave speed. However, the sampling frequency for the measurements was too low to accurately resolve the speed of sound in the present work.
The speed of sound in pure water at 25ºC is about 1500 $m.s^{-1}$. However, the observed oscillations, in combination with the length of the pipe, suggest that the current speed of sound is approximately 80 $m.s^{-1}$. Wylie and Streeter [4] show that the speed of sound can be reduced to the order of 80 $m.s^{-1}$ at a water temperature of 20ºC and a 0.1% volume fraction of air. In the test rig, the air entrainment due to the pumping caused problems when the particle image velocimetry method (PIV) was used. There were too many, and too large, air bubbles in the water. The test rig was modified in order to reduce air entrainment to a minimum, but the problem was not eliminated. The air bubbles were present during the pressure measurements, but reduced before the PIV measurements. It is thus likely that the air content was high enough during the pressure measurements to give a speed of sound in the order of 80 $m.s^{-1}$. The structure of the pipe is as well not perfectly rigid, which also significantly reduces the sound propagation speed. The flexibility of the structure is unknown, but certainly contributes to the low speed of sound in the system.

3. 3D numerical investigations

The experimental results raise the question of the pressure fluctuations during the period when the gate is closed. To understand if the free surfaces have an influence on the pressure fluctuations, the test case is numerically investigated using CFD. The OpenFOAM solver used to compute the flow implements the incompressible Navier-Stokes equations, and includes the free surface in the upper and lower tanks through the Volume Of Fluid (VOF) method. The assumption of incompressibility isolates the effects of the free surfaces by removing the pressure wave propagation. No turbulence model is presently included, but the slight diffusivity of the convection scheme contributes to the modeling of turbulence in the spirit of ILES. The closing gate is modelled using a dynamic mesh library. It features sliding interfaces with mesh topology changes at the mesh surfaces along both sides of the gate, and removal/addition of mesh layers as the gate is moving downwards/upwards. The implementation requires that at least one cell is kept between the gate and the lower boundary.

3.1. Computational domain, mesh and gate motion

Figure 5 shows the computational domain, as well as some feature of the mesh. The mesh is generated in ICEM CFD and consists on 2 million hexahedral cells. The upper and lower tank free surfaces are included in the domain. Two baffles in the bend are resolved. The knife valve below the upstream tank is modeled as a thin baffle that obstructs about 90% of the cross-sectional area of the pipe, generating a pressure loss that corresponds to that estimated from the experimental data in section 2.4. Figure 6 shows the dynamic mesh motion of the gate.

3.2. Case set-up and solution procedure

The experimental flow rate, 50 $l.s^{-1}$, was used to set both the inlet and outlet velocity of the water to/from the upper/lower tanks. The total amount of water in the system is thus kept constant, but the head at the gate is allowed to change due to the varying free surfaces. To start with, the gate was kept open so that the flow would develop in the system, and the upper and lower free surfaces would reach a stable level. The transient is achieved by closing the

gate with a constant speed during 4.9 s (preserving a cell between the gate and the bottom boundary), keeping the gate closed 8 s, and opening the gate with a constant speed during 4.9 s. The time step was set to $\Delta t = 0.0002$ s, yielding a maximum Courant number of Co = 0.2.

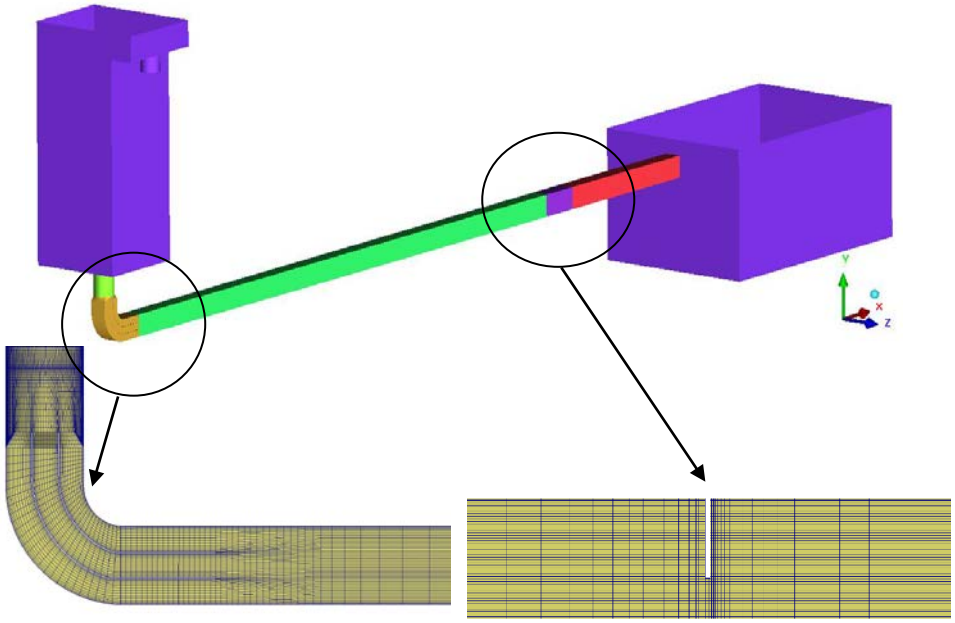

Figure 5: Computational domain and some features of the mesh.

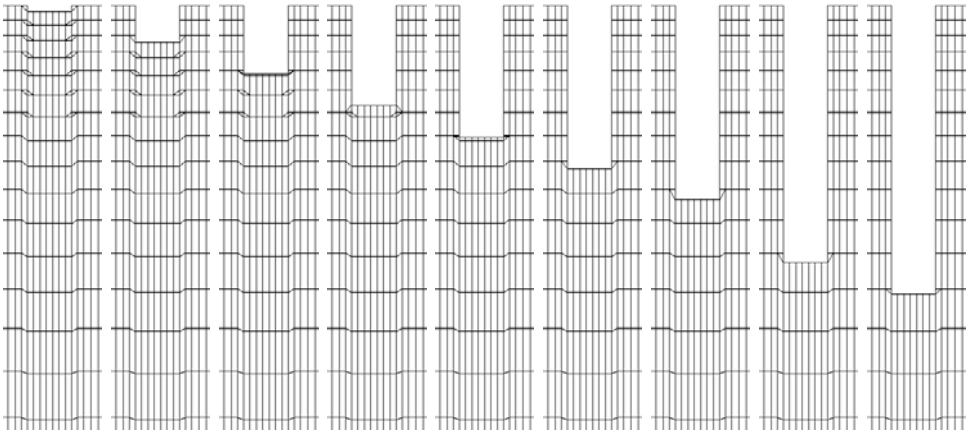

Figure 6: Zoom-up of the mesh at the gate as the gate is closing.

3.3. Results of the 3D numerical simulation

Figure 7 shows the pressure and velocity responses computed by the 3D unsteady incompressible solver. The transient starts at 5 s, after a stabilization period, followed by 4.9 s closing, 8 s closed and 4.9 s opening gate. As the gate closes the pressure increases, supported by a reduction of the minor-loss below the upstream tank as the flow velocity decreases. The pressure increase is about 3.5 10^4 *Pa* in both the experimental and numerical cases, showing that the main behavior of the flow is well captured. When the gate approaches the fully closed position the overshoot of pressure is similar as in the measurement. For the experimental case this is the origin of the pressure wave. For the 3D computation the incompressibility assumption forces the pressure to immediately drop to the hydrostatic pressure. During the period when the gate is closed the pressure increases linearly due to the water level increase in the upstream tank, similar to what is observed experimentally. There are no fluctuations in pressure when the gate is closed, suggesting that the free surfaces are not the cause of the pressure fluctuations observed in the experimental results. When the gate is closed it can be

observed that the velocity at the gate is not totally zero, due to a leakage flow below the gate. The numerically predicted axial velocity variation along a vertical line 50 mm upstream the gate compares very well with the experimental data, see Figure 8.

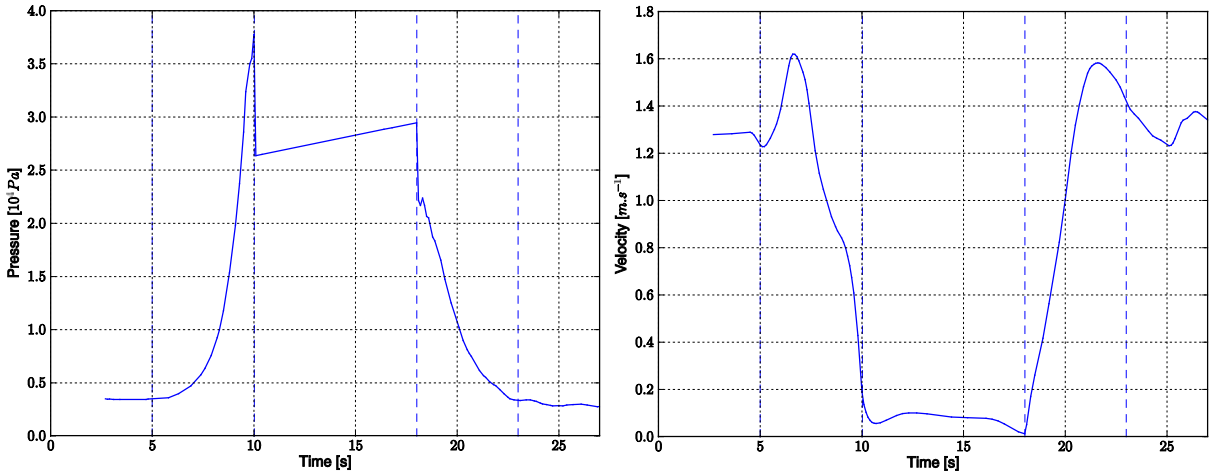

Figure 7: 3D computed pressure (left) and velocity (right) upstream the gate.

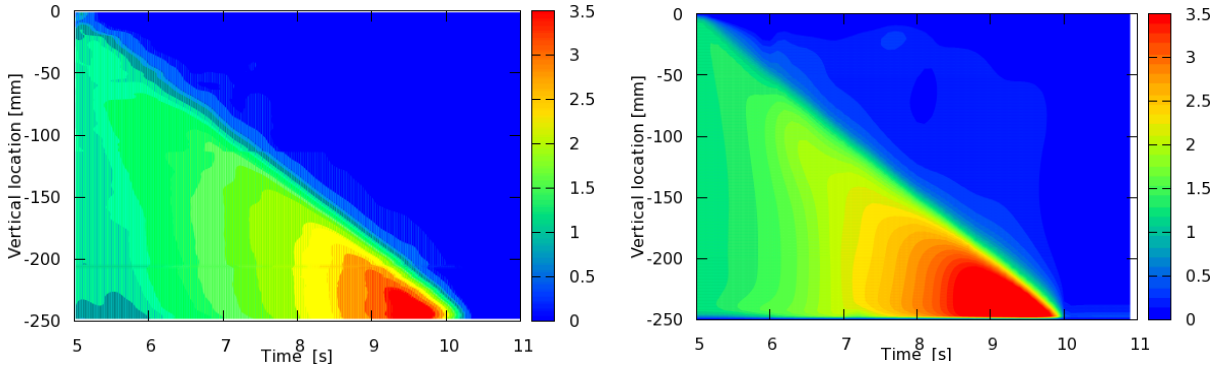

Figure 8: Measured (left) and computed (right) variation of the axial velocity along a vertical line 50 mm upstream the gate in the middle of the pipe as a function of time.

4. 1D numerical investigations

To understand if the sound propagation speed has an influence on the pressure fluctuations, the test case is numerically investigated using Methods of Characteristics (MOC), a mathematical technique for solving hyperbolic partial differential equations. In the present work the MOC is applied to the water hammer equations. The equations are a simplified form of the Navier-Stokes equations, and the sound speed is introduced to consider the flow compressibility. The MOC is the most popular method 1D method for water-hammer in pipeline systems [11], and it is also possible to include tanks with free surfaces [12].

4.1. Computational domain

A reservoir-pipeline-gate system is used to compute the 1D behavior of the flow, see Figure 9. The system is divided into two parts. The first part of the computational domain includes the reservoir, its free-surface, and the vertical pipe. The second part of the domain models the horizontal pipe. The experimentally estimated minor-loss is implemented between the two parts of the domain to take into account the losses induced by the knife valve and the 90º bend. The dynamic losses are however not implemented in the present work. The grid size is 0.08 m, based on the sound speed and the time step to keep the Courant number at one. Thus the vertical pipe is divided into 25 nodes, while the horizontal one is divided into 75 nodes.

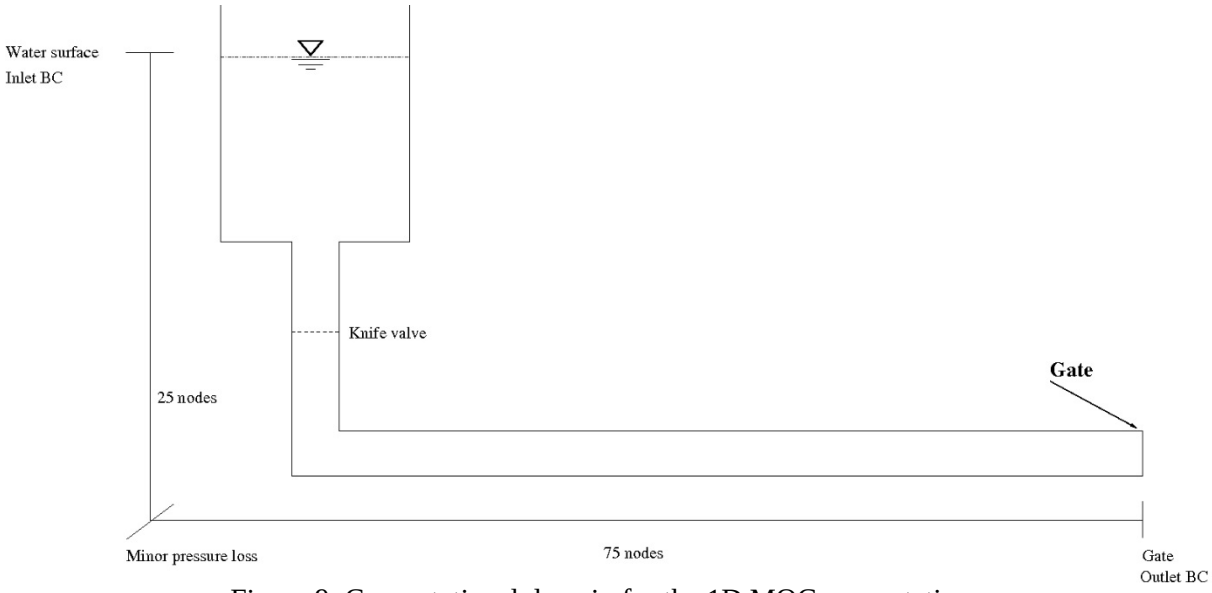

Figure 9: Computational domain for the 1D MOC computations.

4.2. Case set-up

The time step for the 1D computation is set to $\Delta t = 0.001$ s. At the inlet an initial head of H=3 m is specified, as well as the discharge of Q=0.05 $m^3.s^{-1}$. At the outlet, the time-evolution of the discharge is specified in different ways to mimic the characteristics of the gate valve. For the 1D MOC computations, the speed of sound was chosen to be a = 80 $m.s^{-1}$, see section 2.5. The speed of sound was chosen to obtain the same frequency of the pressure fluctuations as the measurements during the period when the gate is closed.

4.3. Results of the 1D numerical simulations

When the gate closes the behavior of the pressure is dictated by the characteristics of the gate. Figure 10 illustrates this using three different discharge evolutions at the outlet boundary in the MOC computation. The pressure response at the gate is compared with the experimental signal. The elliptic discharge characteristic is the implementation that best fits the experimental pressure signal, but it still over-predicts the overshoot of pressure when the gate is closed. The gate discharge characteristic is instead determined from the pressure measurements during the gate closure. Figure 11 shows the calculated discharge at the gate when setting the extracted pressure as the outlet boundary during the gate closure. Figure 12 shows the computed pressure development using the calculated discharge from Figure 11 during the gate closure as outlet boundary condition, and assuming a no-flow condition when the gate is closed. The 1D MOC computation captures well the behavior of the flow, but the pressure waves are not damped as much as in the experiment. This is probably due to a lack of a dynamic pressure loss term in the 1D MOC model.

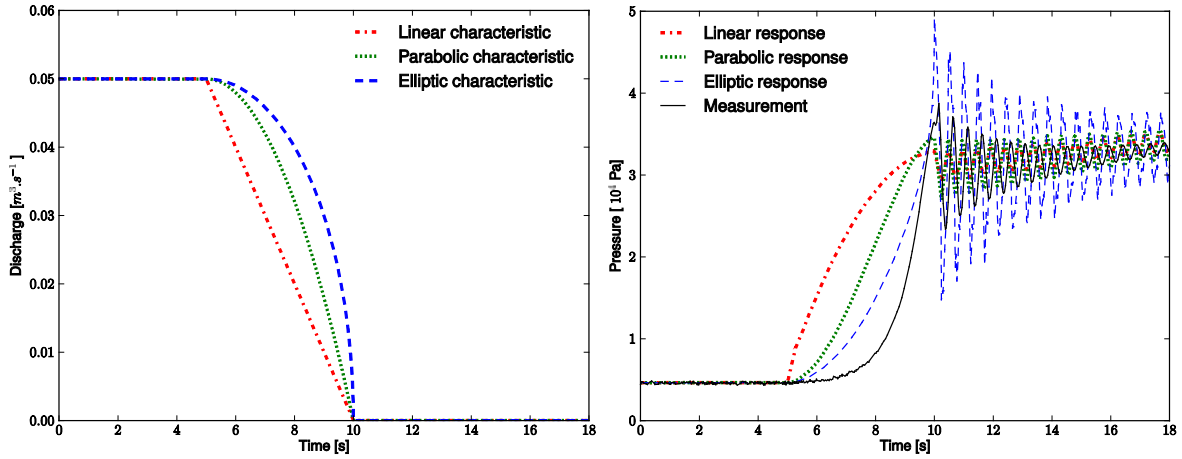

Figure 10: Approximate gate closing characteristic (left) and computed pressure response compared with the measurements (right).

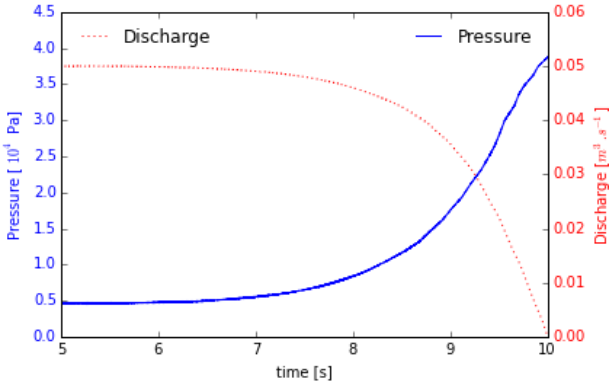

Figure 11: Measured pressure and corresponding approximated discharge, as the gate closes.

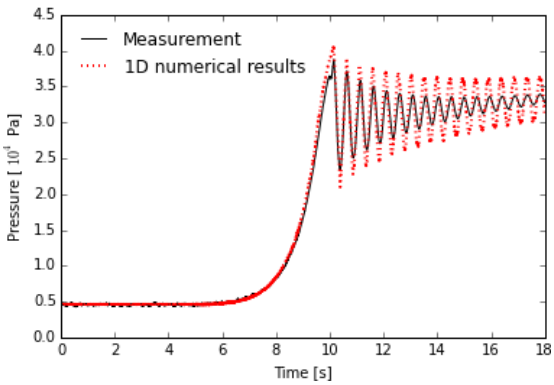

Figure 12: Pressure variations using the experimentally determined gate characteristics.

5. CONCLUSIONS

An experimental rig was designed and manufactured with the purpose of studying the pressure variations and velocity field associated with the closure of a gate in a tunnel at a high Reynolds number. Time-resolved static pressure measurements quantify the increment of the pressure during gate closure and the following pressure fluctuations. PIV measurements show the evolution of the velocity as the gate closes.

The case is studied numerically with two approaches. The result from a 3D incompressible approach with free surfaces captures the main behavior of the flow well except for the pressure fluctuations that correspond to a finite sound propagation speed. It shows that the pressure fluctuations are not due to the free surfaces, and suggests that they are solely due to compressible effects.

It is found that the outlet boundary condition that represents the characteristics of the closing gate in a 1D approach is important to accurately predict both the pressure rise and pressure fluctuations. The hypothesis of a low speed of sound in this work due to a large amount of air in the water and due to the pipe flexibility is investigated. The good agreement between the experimental and numerical results confirms that a speed of sound that corresponds to water with a volume fraction of air of 0.1% is appropriate in the current case.

5. ACKNOWLEDGEMENTS

The research presented was carried out as a part of the ”Swedish Hydropower Centre -SVC”. SVC is established by the Swedish Energy Agency, Energiforsk and Svenska Kraftnät together with Luleå University of Technology, The Royal Institute of Technology, Chalmers University of Technology and Uppsala University, www.svc.nu. The computational facilities are provided by C3SE, the center for scientific and technical computing at Chalmers University of Technology, and SNIC, the Swedish National Infrastructure for Computing.

6. REFERENCES

[1] Fox, J. A, *"Transient flow in pipes, open channels and sewers"*, Textbook, Ellis Horwood Ltd., Chischester, UK, 1989.

[2] Jaeger, C., *"Fluid transients"*, Textbook, Blackie & Sons Ltd., Glasgow, UK, 1977

[3] Tullis, J. P., *"Hydraulics of pipelines - pumps, valves, cavitation, transients"*, Textbook, John Wiley & Sons Inc., New York, NY, USA, 1989.

[4] Wylie, E. B., and V. L. Streeter, *"Fluid transients"*, Textbook, Feb Press, Ann Arbor, MI, USA, 1982.

[5] Miller, D. S., *“Internal Flow Systems”*, BHRA Information Services, Bedford, UK, 1990.

[6] Idelchik, I.E., *“Handbook of Hydraulic Resistance”*, 3rd ed., Begell House Inc., New York, NY, USA, 1996.

[7] Adamkowski, A., *“Case study: Powerplant penstock failure”*, J. Hydraulic Eng., Vol. 27, 2001, pp. 547-555.

[8] Jiménez, O. F., and M. H. Chaudhry, *“Stability of hydroelectric power plants”*, J. Energy Eng., Vol. 113, 1987, pp. 50-60.

[9] Ramos, H., and A. B. Almedia, *“Dynamic orifice model on waterhammer analysis of high or medium heads of small hydropower schemes”*, J. Hydraulic Res., V. 39, 2002, No. 2, pp. 429-436.

[10] Yu, X., J. Zhang, and A. Hazrati, *“Critical superposition instant of surge waves in surge tank with long headrace tunnel”*, Can. J. Civ. Eng., Vol. 38, 2011, pp. 331-337.

[11] Zhao, M., and Ghidaoui, M. S. (2004). “Godunov-type solutions for water hammer flows.” J. Hydraul. Eng., 10.1061/(ASCE)0733-9429(2004),130:4(341), 341–348.

[12] Wang, C. and Yang, J.D, *“Water Hammer Simulation using Explicit-Implicit Coupling Methods”*, J. Hydraul. Eng., 141(4), 04014086. 10.1061/(ASCE)HY.1943-79000000979, 2014.